Journal of Life Sciences and Biomedicine, vol. 1 (74), No 1, p. 29-36 (2019)

Resolution and resolvability in one, two and three dimensions

G.M. Gasimova[1,2]*, R.C. Masmaliyeva[1], G.N. Murshudov[1,3]*****

[1]*Institute of Molecular Biology & Biotechnologies, Azerbaijan National Academy of Sciences, Azerbaijan*
[2]*Azerbaijan State Oil and Industry University, 34 Azadliq ave., Baku AZ1010, Azerbaijan*
[3]*MRC Laboratory of Molecular Biology, Cambridge, UK*
** For correspondence: GXG557@alumni.bham.ac.uk*
*** For correspondence: r.masmaliyeva@gmail.com*
****For correspondence: garib@mrc-lmb.cam.ac.uk*
Accepted for publication: 10 August 2019

This contribution describes an approach to the problem of resolution and resolvability in scattering methods (*e.g.* X-ray diffraction, electron microscopy) in the presence of series termination and blurring. One-, two- and three-dimensional cases are considered separately. Formulas relating the effects of nominal resolution and blurring to peak resolvability are derived and analysed. We show that both blurring and series termination widen point source peaks thus reducing their resolvability.

Keywords: *Refinement, electron cryo-microscopy, Fourier shell correlation, Fourier transformation, Gaussian distribution*

INTRODUCTION

Macromolecular crystallography (MX) and single particle cryo electron microscopy (cryo-EM) are two widely used scattering methods used to derive atomic models of biological molecules (Rupp, 2010; Frank, 2005). Both techniques produce density maps that are interpreted as atomic models (Emsley and Cowtan, 2006). Derived atomic models are deposited to the Protein Data Bank (PDB) via which they are made available to the community free of charge (Berman et al., 2002). Maps can be represented equivalently either in image space as a function sampled on a regular three-dimensional grid points or as Fourier coefficients of these maps. In crystallography observations are related to the Fourier coefficients (Harker and Kasper, 1948), whereas in cryo-EM usually observations are made for images themselves (Frank, 2005). Details that can be seen in these maps and therefore accuracy of atomic models depend on the amount and quality Fourier coefficients.

There are some confusion and controversy on the definition and use of resolution concept: current definition only uses the highest frequency terms of the Fourier coefficients used for map calculations (Wlodawer et al., 2017). This definition does not account for the noise in the data, absolute and relative mobility of the objects under study. It only states the radius of a sphere within which observations reside. Although it does seem that in crystallography, since observations are directly related to the Fourier coefficients, the highest observed frequency term should define the resolution provided that all Fourier coefficients have been measured with high accuracy. This definition has been successfully used for last 100 years. However now increasingly more and more noisy data are used for structure determination and old definition is no longer applicable: this definition only defines the radius in the Fourier space where data reside. Another problem arises when the resolution of structure used as an indication of their accuracies and different structures are compared with reference to resolution; e.g. for selection of the “best” atomic models, for comparison of accuracy of atomic models to typical models in the PDB corresponding to the same resolution.

In cryo-EM resolution is defined by analogy to that in crystallography: the highest frequency of observed Fourier coefficient are defined for which Fourier shell correlation (fsc) is more than 0.143 where fsc is calculated in narrow shells between Fourier coefficients of two independently reconstructed maps (Rosenthal and Henderson, 2003;

Scheres, 2012). Both of these definitions, to a certain degree, make use of the signal to noise ratio. Information about the signal-noise ratio should also be used in structure determination and refinement (Murshudov, 2016). Usage of the highest observed significant frequency terms as a definition of the resolution does not account for the behaviour of the noise and the signal over the Fourier space: it is time to make these definitions more precise that accounts for the quality of all available information in the data.

Moreover, both of these definitions do not fully account for the signal the noise level in the data, they also do not use the fact that molecules oscillate resulting in the blurred image and therefore reducing the visibility of them in the map affecting different parts of the density differently in accordance with varying mobility of molecules.

In this paper, we will address this problem theoretically with some certain simplifying assumptions that make calculations manageable. Here we consider one-, two- and three-dimensional cases and show that objective measure can be calculated to measure resolvability that would reflect the information contained in the data about the object under study.

1. Resolution and Resolvability

Let us assume that we have observations in the Fourier space up to a nominal resolution s_{nom}. Our observations are Fourier coefficients that are sum of two components $F_{obs}(s)$=$F_{true}(s) + F_{noise}(s)$, where $F_{obs}(s)$ is observed, $F_{true}(s)$ is the "true" and $F_{noise}(s)$ is the noise Fourier coefficients. We also assume that "true" image is a blurred version of the object we would like to observe, where blurring is linear. *I.e.* true part of the observed image is:

$$\rho_{true}(x) = \int_y \rho_0(y) g(x,y) dy \quad (1)$$

where *g(x,y)* is a blurring function that is normalised everywhere:

$$\int_y g(x,y) dy = 1 \quad (2)$$

where $\rho_{true}(x)$ is the true image, $\rho_0(x)$ is the image we would like to observe.

Basic image processing and modelling problem is that our data have noise and blurred then we would like to solve the equation (1) so that as much as possible details in the map can be visualised and modelled. This problem can be considered as Wiener filtering problem (Vega and Rey, 2012). In general, a solution of the equation (1) requires solving very large linear systems which is not possible in practice. In addition, since we do not know the blurring function then the problem becomes even more complex; we must find blurring function as well as solving the equation (1). When blurring is position independent, *i.e.* $g(x,y) = g(x-y)$ then the problem becomes simpler, "true" image is just a convolution of the unblurred image with the blurring function. In this case, it is known that $F_{blur}(s) = F_0(s)F_g(s)$, i.e. Fourier coefficients of the blurred image is the product of Fourier coefficients of the unblurred image and that of blurring function.

So, the observation in the Fourier space can be written as:

$$F_{obs}(s) = F_0(s)F_g(s) + F_{noise}(s)$$

Recall that our observations are within the nominal resolution sphere $|s| < s_{nom}$. We assume that we know the blurring function - $F_g(s)$, the variance and covariance of the noise in the Fourier space - F_{noise}. We want to know what are the details in the image that can be seen (distinguish from each other) for a given nominal resolution, blurring function and noise level. We will approach to this problem step by step. First, we will assume that there is no noise $F_{noise}(s) = 0$, no blur $F_g = 1$ and the only shortcoming of our observations is that we observe only within a resolution sphere $|s| < s_{nom}$, the only problem is the series termination effect. After analysis of this problem we will move on to assume that there is a position independent blurring and we know blurring function. We also will assume that the blurring function is Gaussian and we know the blurring parameter. Then we will consider the cases when there is noise and we know the variance and covariance of the noise. Then we assume that we do know the shape of blurring function but we do not know its parameters (e.g. blurring is Gaussian but we do not know variance of the Gaussian). Our problem then will be a) what level of details can be seen; b) what are the optimal parameters of blurring function. Then we will move on and assume that blurring is position dependent. However, in this work we will

only consider only limited resolution data (series termination effect) and position independent Gaussian blurring. Remaining problems will be dealt with in future works.

To define the resolvability in the scattering data we will assume that there are two point sources, however because of observational deficiencies or intrinsic properties, *e.g.* mobility of the objects observed sources are broadened. We will consider two reasons for peak broadening: a) our observations are within a certain resolution limit - $|s| < s_{nom}$; b) sources oscillate during observations and we observe blurred version of these sources.

We will define resolvability as follows: With a given nominal resolution limit, blurring and noise level resolvability is the minimum distance between like point sources that can be distinguished in the map.

We assume that we have two point sources in n-dimensional space and they are blurred by a Gaussian blur with the variance $u = \frac{B}{8\pi^2}$. Then the observed peak for one point source would have the form:

$$f_B(x) = \int_{|s|<s_{nom}} e^{-\frac{B|s|^2}{4}} e^{i2\pi xs} ds \qquad (3)$$

where integral is in n-dimensional space. *xs* is the bilinear form formed with the vectors in image (x) and Fourier space (s), $i = \sqrt{-1}$ is the imaginary number. We would like to find minimal non-zero root of this equation:

$$f_B(0) + f_B(x) - 2f_B\left(\frac{x}{2}\right) = 0 \qquad (4)$$

i.e. we want to find such a distance between point sources that image values at the positions of the peaks are bigger than in the middle of the vector connecting them.

In the following sections, we will consider this equation for one, two and three dimensions with and without blurring.

2. Peak widening and resolvability in 1D

Let us assume that we have a point source: $\delta(x)$ in one dimensional case. Its Fourier transformation for all s $F(s) = 1$. Now let us assume that we cut the data $s \in [-s_{nom}, s_{nom}]$. Let us calculate the inverse Fourier transformation which is the following integral:

$$f_0(x) = \int_{-s_{nom}}^{s_{nom}} e^{i2\pi xs} ds = \frac{2s_{nom}\sin(2\pi xs_{nom})}{2\pi xs_{nom}} =$$
$$= 2s_{nom} j_0(2\pi xs_{nom}) \qquad (5)$$

Therefore, in this case, the above stated problem is reduced to the solution of the equation:

$$2s_{nom} + 2s_{nom} j_0(2\pi xs_{nom}) -$$
$$-4s_{nom} j_0(2\pi xs_{nom}/2) = 0 \qquad (6)$$

If we let $y = 2\pi xs_{nom}$ then the solution of (6) is equivalent to finding of the smallest non-zero root of the equation

$$1 + j_0(y) - 2j_0(y/2) = 0 \qquad (7)$$

Solution of this equation is $y_0 = 4.28$ and therefore $x_0 = \frac{y_0}{2\pi s_{nom}} = \frac{0.68}{s_{nom}}$.

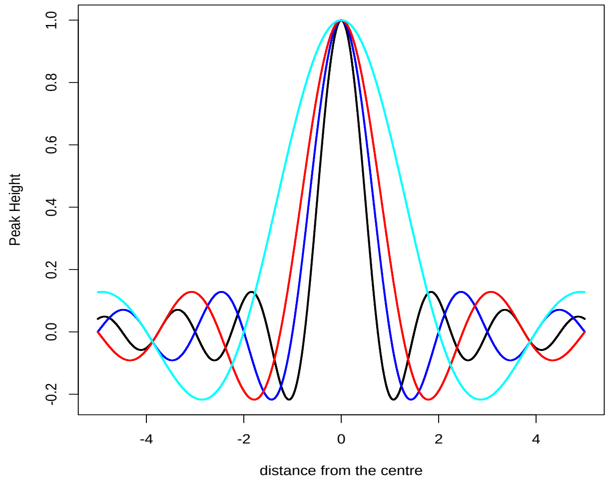


Fig. 1. The graphs of $f(x) = j_0(2\pi xs_{nom})$ function for different values of nominal resolution - s_{nom}. This graph shows that peaks are broadened as s_{nom} decreases. Black line corresponds to $s_{nom} = 0.75$, blue line corresponds to s_{nom} =0.5, red line corresponds to $s_{nom} = 0.4$ and cyan line corresponds to $s_{nom} = 0.25$.

Figure 1 demonstrates the effect of nominal resolution on peak broadening. As it is expected as the nominal resolution increases the calculated peaks become sharper.

If we have two point-sources and observations inside the interval $|s| < s_{nom}$ what is the minimal distance between peaks so that they can be seen as a separate peak. Let us assume that distance between point sources is z. Then we can plot the following function:

$$j_0(2\pi xs_{nom}) + j_0(2\pi(x - z)s_{nom})$$

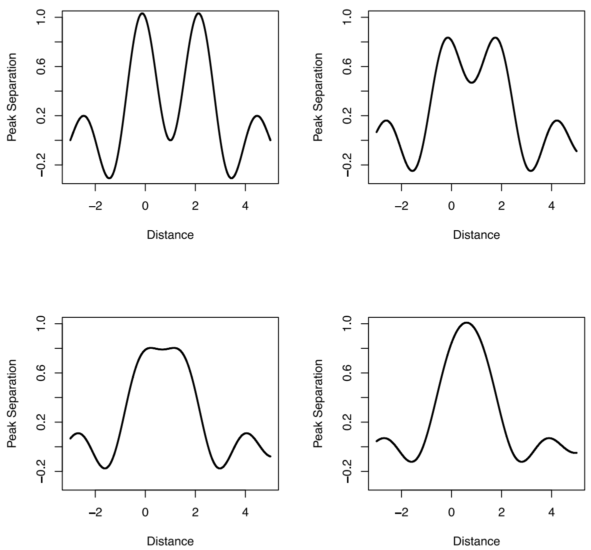


Fig. 2. The graph of two point-sources for one-dimensional case – the function $j_0(2\pi x s_{nom}) + j_0(2\pi(x - z)s_{nom})$. Resolution is s_{nom}=0.5. Top left: distance between sources is 2Å, top right: distance between source is 1.6Å, bottom left: distance between sources 1.36Å, bottom right: distance between sources is 1.2Å

Fig. 2. demonstrate that inside $|s| < 0.5Å^{-1}$ interval when the distance between peaks are decreasing then resolvability power of the map become is reduced. When the distance is 2Å then peaks are clearly visible, when the distance becomes 1.6Å peaks become less separable, when the distance between peaks is 1.36Å then peaks are marginally separable and when the distance is 1.2Å then two peaks are merged together and they are no longer be seen as two different peaks. It should be noted that when the distance is equal to the resolvability – 1.36Å then, although peaks can still be separated they come close to each other - the maxima of peaks are no longer at the original peak positions.

Gaussian blurred source with the variance $u = \frac{B}{8\pi^2}$ has the form:

$$\rho(X) = 2\sqrt{\frac{\pi}{B}} e^{-\frac{x^2}{B}} \qquad (8)$$

Fourier transformation of this source is:

$$F(s) = e^{-B|s|^2/4} \qquad (9)$$

Now we again assume that the data have been observed within the interval $s \in [-s_{nom}, s_{nom}]$. Inverse Fourier transformation of the Gaussian blurred point source is:

$$f_B(x) = \int_{-s_{nom}}^{s_{nom}} e^{-B|s|^2/4}\, e^{i2\pi xs} ds \qquad (10)$$

resulting in

$$f_B(x) = 2\frac{\sqrt{\pi}}{\sqrt{B}} e^{-\frac{(2\pi x)^2}{B}} Re(\mathrm{erf}(\frac{\sqrt{B}s_{nom}}{2} - \frac{i2\pi x}{\sqrt{B}}))$$

We can evaluate this function if we have access to the error function of complex variables. This function can be evaluated efficiently using Faddeeva function (Poppe and Wijers, 1990) defined for complex arguments as:

$$\omega(z) = e^{-z^2} erfc(-iz) = e^{z^2}(1 - erf(-iz))$$

where z is a complex variable and the values of this function, in general, are complex numbers.

Using the relationships between error and Faddeeva functions we can write:

$$f_B(x) = 2\frac{\sqrt{\pi}}{\sqrt{B}} e^{-\frac{(2\pi x)^2}{B}} - 2\frac{\sqrt{\pi}}{\sqrt{B}} e^{-\frac{Bs_{nom}^2}{4}} Re(e^{i2\pi x s_{nom}} w\left(\frac{2\pi x}{\sqrt{B}} + i\frac{\sqrt{B}s_{nom}}{2}\right))$$

Let us compare the effects of different B values on point source broadening.

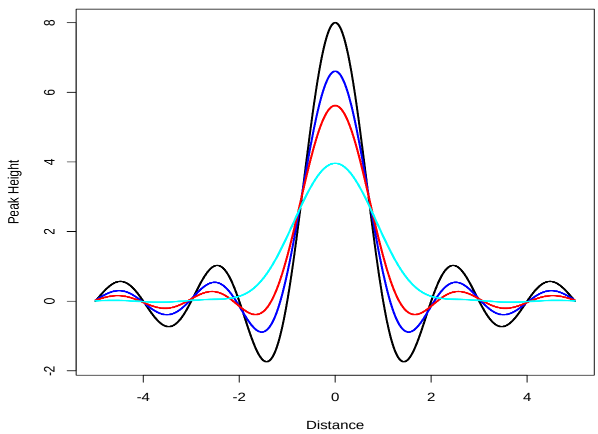


Fig. 3. Point source with blurs**.** All plots correspond to s_{nom} = 0.5, Black line corresponds to B = 0.001Å^{-2}, blue line corresponds to B = 10Å^{-2}, red line corresponds to B=20Å^{-2} and cyan line corresponds to B=50Å^{-2}.

It is clear that as B value increases the peaks are broadening thus reducing resolvability of these peaks. To observe highly oscillating peaks one needs to produce maps with as little as possible noise.

Fig. 4 shows that for the same resolution and distance between Gaussian sources as blurring parameter increases peaks become less and less resolvable. It should be noted that if there would be no noise and blurring parameter would be known then we could remove the effect of blurring without difficulty by simply using deconvolution. The problem becomes more complicated when the noise comes into play. All observations in reality are with noise, the noise level can be reduced it is impossible to remove it completely.

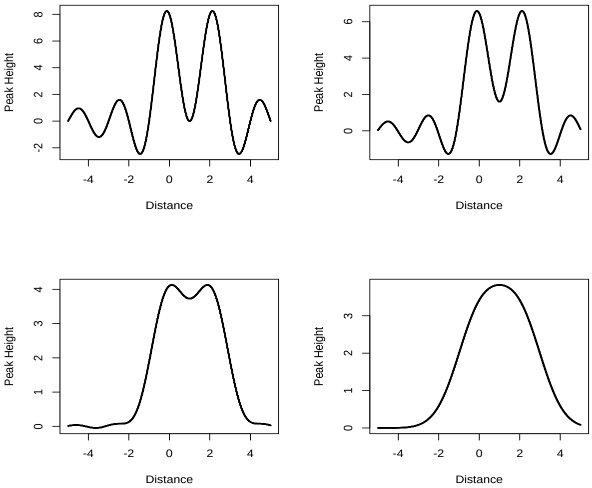


Fig. 4. Sum of two Gaussian blurred sources at $s_{nom} = 0.5, dist = 2$Å for different blurring parameters. Top left: B=0.01Å^{-2}, top right: B=10Å^{-2}, bottom left B=50Å^{-2}, bottom right B=100Å^{-2}.

3. Peak widening and resolvability in 2D

Now let us assume that we have a point source in two dimensions. Its Fourier transformation for all s is constant. Now let us assume that we cut the data within $|s| < s_{nom}$. The observed peak will have the form:

$$f_0(x) = \int_{|s|<s_{nom}} e^{i2\pi xs} ds = = 2\pi s_{nom}^2 \frac{J_1(2\pi|x|s_{nom})}{2\pi|x|s_{nom}} \quad (11)$$

where J_1 is the 1st order Bessel function of first kind. All other terms are the same as defined above. Since $\lim_{t\to 0} \frac{J_1(t)}{t} = \frac{1}{2}$ we can write $f_0(0) = \pi s_{nom}^2$. If we use $t = 2\pi|x|s_{nom}$ then the equation (4) is reduced to:

$$1 + \frac{J_1(t)}{t} - 2\frac{J_1(t/2)}{t/2} = 0 \quad (12)$$

The solution of this equation is $t_0 \approx 4.7715$ and we obtain that: $t_0 = 2\pi s_{nom} x$ and therefore in the absence of blurring resolvability in two-dimensional case is: $x_0 = \frac{t_0}{2\pi s_{nom}} = 0.7594\frac{1}{s_{nom}}$. Since these functions have qualitatively the same form as in one-dimensional case we do not show figures for unblurred cases in two dimensions.

The observed peak with the blurring parameter B and nominal resolution s_{nom} is calculated using the following integral:

$$f_B(x) = = \int_0^{2\pi} \int_0^{s_{nom}} e^{-B|s|^2/4}|s|\cos(2\pi|x||s|\cos(\phi))d\phi ds$$

To our knowledge there is no closed form expression for this integral, therefore this integral is calculated numerically using the statistics package R (R core team, 2018) that uses QUADPACK for numerical integration (Piessens et al., 1983).

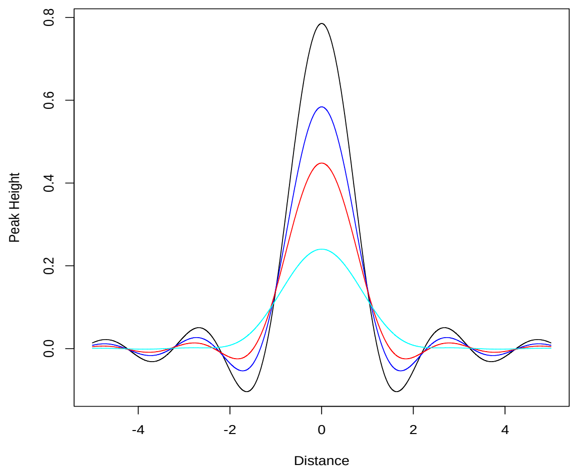


Fig. 5. Point source with blur in 2D, $s_{nom} = 0.5$Å^{-1}. Black line corresponds to B = 0.001, for blue line B = 10, for red line B=20 and for cyan line B=50.

The figure 5 illustrates that for a given resolution the observed peaks are broadened as blurring increases.

Again, as in one-dimensional case, let us consider the blurred image with two point sources and with the observations within the circle $|s| < s_{nom}$. We assume that the distance between these point sources is z. Now we can plot the following function:

$$f_B(2\pi x s_{nom}) + f_B(2\pi(x - z)s_{nom})$$

to see how peaks widen and become unsolvable as blurring parameter increases (figure 6).

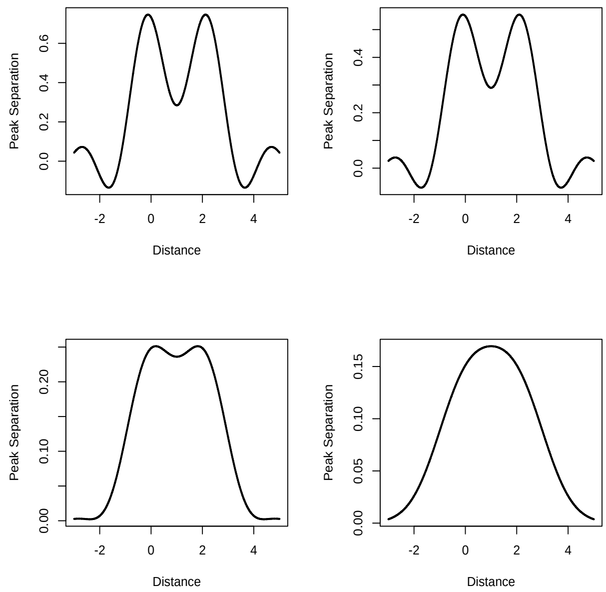


Fig. 6. The graph of two point sources in two dimensions with resolution $s_{nom} = 0.5Å^{-1}$ and distance between sources $d = 2.0Å$ for different blurring parameters. Top left: B=0.01Å^{-2}, top right: B=10Å^{-2}, bottom left B=50Å^{-2}, bottom right B=100Å^{-2}.

The Figure 6 illustrates again that in two dimensions also as blurring parameter – B increases peaks become less and less resolvable.

4. Peak widening and resolvability in 3D

Now let us consider three-dimensional case with point sources. Peaks for which Fourier coefficients observed within a nominal resolution will have the form:

$$f_0(x) = \int_{|s|<s_{nom}} e^{2\pi ixs} ds = 4\pi \frac{-2\pi|x|s_{nom}\cos(2\pi|x|s_{nom}) + \sin(2\pi|x|s_{nom})}{(2\pi|x|)^3} = \frac{4\pi s_{nom}^3 j_1(2\pi|x|s_{nom})}{2\pi s_{nom} x}.$$

where j_1 is the spherical Bessel function of first order. All other notations are the same as defined above.

In this case, the solution of equation (4) gives: $x_{res} = \frac{0.8322}{s_{nom}}$. It is the maximum attainable resolvability in three dimensions in the absence of blurring. We will consider blurring with various parameters, although in this case the results will be qualitatively similar to one- and two-dimensional cases. Indeed, it can be seen in figure 7 and 8.

We next consider the case when the density is blurred with a Gaussian blurring function with the parameter B. To add the effect of blurring we again need to calculate the integral:

$$f_B(x) = \int_{|s|<s_{nom}} e^{-\frac{B|s|^2}{4}} e^{(2\pi ixs)} ds$$
$$= \left(\frac{8\pi}{B}\right)^{\frac{3}{2}} e^{-\frac{(2\pi|x|)^2}{B}} - e^{-\frac{Bs_{nom}^2}{4}} \left(\frac{4\sin 2\pi|x|s_{nom}}{|x|B} + \right.$$
$$\left. + \left(\frac{8\pi}{B}\right)^{\frac{3}{2}} Re\left(e^{i2\pi|x|s_{nom}} w\left(\frac{2\pi|x|}{\sqrt{B}} + i\frac{\sqrt{B}s_{nom}}{2}\right)\right)\right)$$

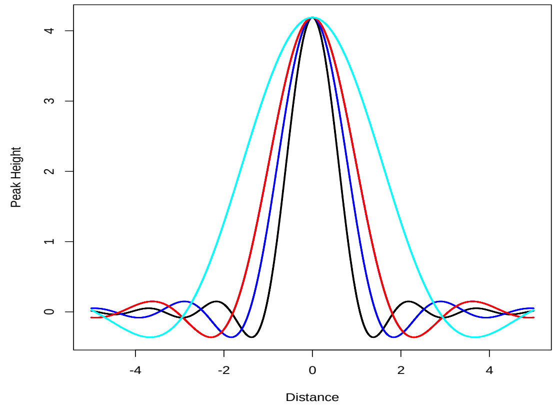


Fig. 7. Peak broadening in the case of no blurring corresponding to different nominal resolution. These graph shows peaks are broadened as s_{nom} decreases. Black line corresponds to $s_{nom} = 0.75$, blue line s_{nom} =0.5, reac line $s_{nom} = 0.4$ and cyan line $s_{nom} = 0.25$.

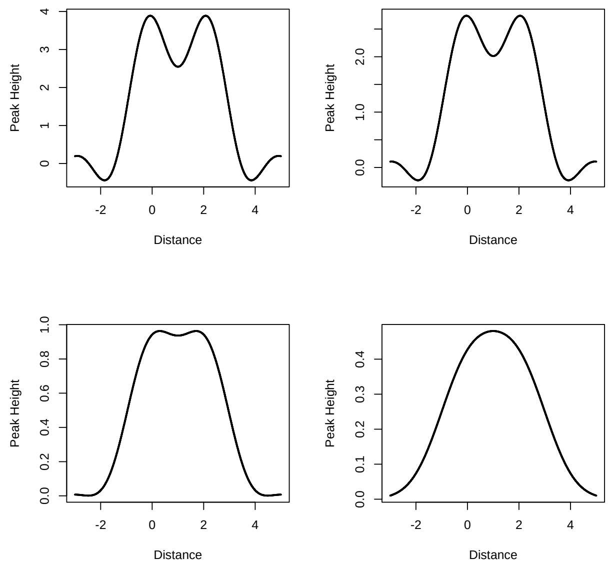


Fig. 8. Sum of two peaks for three-dimensional case with Gaussian blurring. Top left corresponds to B=0.001Å^{-2}, top right corresponds to B=10Å^{-2}, bottom left corresponds to B =50Å^{-2} and bottom right corresponds to B=100Å^{-2}

All terms and variables are as defined before. The first term on the right side of this equation is the peak if there is no series termination and the second terms accounts for the series termination.

Again, we need to plug in this function into the equation (4) and solve it. As expected as B values increase the solution of this equation gives larger and larger distances meaning that when amplitude of blurring increases the resolvability of peaks decreases.

Again, the figure 8 shows that as blurring amplitude increases peak separability and therefore resolvability decreases. Detailed analyses of cases with noise and anisotropic mobility will be the subject of future study.

Conclusion and Future Perspectives

In this work, we presented an approach to the problem of resolution and resolvability for scattering methods used in macromolecular structural biology. We focused on the cases without noise. We assumed that there are only two shortcomings of the observations: 1) diffraction limit, i.e. observations are made within the nominal resolution $|s| < s_{nom}$; 2) sources for which we are doing observations are oscillating and as a result we observe a blurred version of the object. We considered both cases for one-, two- and three-dimensional cases. We showed that as resolution decreases peaks get broader and thus becoming less resolvable as expected. We also found a closed form relationship between the nominal resolution and peak resolvability for one-, two- and three-dimensional cases. Similar effects are observed when objects are blurred with a Gaussian function – peaks get broader as the amplitude of oscillation increases and they become less resolvable. It has already an implication to structural biology that signal level in different parts of the observed density will be different and will correspond to the amplitude of oscillation of the molecule corresponding to these parts of the density.

Future work will focus on a theoretical treatment of the effect of noise on the peak resolvability. Ultimate purpose of this work, that will be dealt in future works, is to derive an algorithm to calculate position and orientation dependent resolvability in the density corresponding to noisy data with anisotropic signal strengths. The planned work will answer to one of the long-standing questions in structural biology: what are the details that can be observed in the map if we do know the nominal resolution, the noise level, relative and absolute amplitudes of mobility for different parts of the calculated (observed) maps. The result of this work will help the unification of resolvability used in different scattering methods. However, we would like to stress that our main concern is macromolecular crystallography and single particle cryo-electron microscopy.

ACKNOWLEDGEMENTS

We would like to thank Laboratory of Computational Structural Biology, Institute of Molecular Biology and Biotechnologies of ANAS. Part of this work was supported by Presidium of Azerbaijan National Academy of Sciences grant of decree № 5/9 dated on 15.03.2017. GNM also thanks **MRC grant MC_US_A025_0104**. We would also like to thank to Prof. Irada Huseynova for her support.

REFERENCES

Berman H.M., Battistuz T., Bhat T.N. et al (2002) The Protein Data Bank. *Acta Crystallogr.*, **D58**: 899-907.

Rupp B. (2010) Biomolecular crystallography: principles, practice and applications to structural biology. Abingdon, New York: Garland Science, Taylor & Francis Group, Pp. 808.

Emsley P., Cowtan K.D. (2004) Coot: model-building tools for molecular graphics. *Acta Crystallogr. D*, **60:** 2126-2132.

Harker D., Kasper J.S. (1948) Phases of fourier coefficients directly from crystal diffraction data, *Acta Cryst.*, **1:** 70.

Frank, J (2005) Three-dimensional electron microscopy of macromolecular assemblies: visualization of biological molecules in their Native state. New York, Oxford University Press.

Murshudov G.N. (2016) Refinement of atomic models against cryoEM maps. *Methods in Enzymology*, **579:** 277-305.

Piessens R., de Doncker-Kapenga E., Uberhuber C., Kahaner D. (1983) Quadpack: a Subroutine Package for Automatic Integration. Springer Verlag.

Poppe G.P.M., Wijers C.M.J. (1990) More efficient computation of the complex error function. *ACM Transactions on Mathematical Software*, **16:** 38-46.

Rosenthal P.B., Henderson R. (2003) Optimal determination of particle orientation, absolute hand, and contrast loss in single-particle electron cryomicroscopy. *J. Mol. Biol.*, **333:** 721-745.

Scheres S.H.W. (2012) RELION: Implementation of a Bayesian approach to cryo-EM structure determination. *Journal of Structural Biology*, **180(3):** 519-530.

R Core Team (2018) R: A Language and Environment for Statistical Computing. R Foundation for Statistical Computing, Viena, Austria.

Vega L.R., Rey H. (2012) A Rapid Introduction to Adaptive Filtering, 7 Springer Briefs in Electrical and Computer Engineering.

Wlodawer A., Li M., Dauter Z. (2017) High-resolution cryo-EM maps and models: A crystallographer's perspective. *Structure*, **25:** 1587-1597.

Bir-, iki və üçölçülü fəzalarda ayırdetmə və ayırdetmə qabiliyyəti

G.M. Qasımova[1,2], R. Ç. Məsməliyeva[1], Q. N. Mürşüdov[1,3]

[1] AMEA Molekulyar Biologiya və Biotexnologiyalar İnstitutu
[2]Azərbaycan Dövlət Neft və Sənayə Universiteti
[3] TTM Molekulyar Biologiya Laboratoriyası, Kembric, Böyük Britaniya

Bu məqalə difraksiya məhdudluğu və bulanıqlıq mövcud olan hallarda səpilmə eksperimental metodlarının (məsələn, kristal diffraksiyası, elektron mikroskopiyası) ayırdetmə və ayırdetmə qabiliyyəti probleminə bir yanaşmaya həsr olunur. Birölçülü, ikiölçülü və üçölçülü halların hər biri ayrı-ayrılıqda nəzəri analiz edilmişdir. Nominal ayırdetmə bulanıqlıqdan asılı olan zirvə ayırdetmə qabiliyyətinin ifadələri alınmış və tədbiq olunmuşdurlar. Biz difraksiya məhdudluğu və bulanıqlıq böyüdükcə nöqtə mənbələrinin bir-birindən ayrı görünməsinin çətinləşdiyini göstərdik.

Açar sözlər: *Saflaşdırılma, elektron kriomikroskopiyası, Furye qabığının korrelyasiyası, Furye çevirməsi, Qauss paylanması*

Разрешение и разрешимость в одном, двух и трех измерениях

Г.М. Гасымова[1,2], Р.Дж. Масмалиева[1], Г.Н. Муршудов[1,3]

[1] Институт молекулярной биологии и биотехнологий НАН Азербайджана
[2] Азербайджанский государственный нефтяной и промышленный университет
[3]MRC Лаборатория молекулярной биологии, Кембридж, Великобритания

В этой статье описывается подход к проблеме разрешения и разрешимости в методах рассеяния (например, дифракция рентгеновских лучей, электронная микроскопия) при наличии разрыва ряда Фурье и размытия. Одно-, двух- и трехмерные случаи рассматриваются отдельно. Получены и проанализированы формулы, связывающие эффекты номинального разрешения и размытия с максимальной разрешающей способностью. Мы показываем, что как размытие, так и разрыв ряда Фурье расширяют пики точечного источника, тем самым снижают их разрешающую способность.

Ключевые слова: *Уточнение, электронная крио-микроскопия, корреляция оболочек Фурье, преобразование Фурье, распределение Гаусса*